ISSN 1062-8738, Bulletin of the Russian Academy of Sciences. Physics, 2014, Vol. 78, No. 12, pp. 1308–1312. © Allerton Press, Inc., 2014.
Original Russian Text © I.V. Timofeev, S.Ya. Vetrov, 2014, published in Izvestiya Rossiiskoi Akademii Nauk. Seriya Fizicheskaya, 2014, Vol. 78, No. 12, pp. 1599–1603.

# Spectral Manifestation of an Effective Refraction Index in a Chiral Optical Medium inside a Fabry–Perot Resonator with Anisotropic Mirrors

**I. V. Timofeev[a, b] and S. Ya. Vetrov[a, b]**

[a] *Faculty of Physics, Kirensky Institute of Physics, Siberian Branch, Russian Academy of Sciences, Krasnoyarsk, 660036 Russia*

[b] *Faculty of Physics, Siberian Federal University, Krasnoyarsk, 660041 Russia*

*e-mail: tiv@iph.krasn.ru*

**Abstract**—New boundary conditions for the decoupling of elliptically polarized eigenmodes in an anisotropic optical cavity are proposed. It is shown that twisting the optical axis changes the phase shift of the waves. The difference between the effective refraction indices is greater than the one between ordinary and extraordinary refraction indices.

**DOI:** 10.3103/S1062873814120296

## INTRODUCTION

As is well known, the pixels of a liquid-crystal display allow us to control the transmission of light via the helical twisting of the optical axis of a liquid crystal (LC). The polarization of the transmitted light rotates around the optical axis due to the Maugin waveguide mode [1]. The phase shift of a wave with rotating polarization contains dynamic and geometric phases [2, 3]. In order to measure the phase shift experimentally, the system is placed into an optical resonator of Fabry–Perot type [4].

Spectral transmission peaks are formed at whole number $N$ of wave periods per resonator cycle $2L$:

$$2n_{\text{eff}}L = N\lambda_0, \tag{1}$$

where $\lambda_0$ is the wavelength in a vacuum and $n_{\text{eff}}$ is the effective refraction index (RI). However, measurements are complicated by the anisotropic medium of the resonator generating two sets of peaks with polarizations along the main axes of the dielectric permittivity tensor and different effective RIs ($n_{\text{eff}}$, $n'_{\text{eff}}$). Rotation of the main axes makes resonant polarizations elliptical, results in mode coupling upon reflection from mirrors, and is manifested as quasi-interaction between normal frequencies (avoided crossing) [5].

In this work, we propose using the anisotropic mirrors of a resonator to suppress mode coupling. It is first noted that twisting amplifies anisotropy. In other words, effective RIs differ from one another more strongly than do ordinary ($n_o$) and extraordinary ($n_e$) RIs. This is in contrast to the formula RI $n_{\text{avg}}$ for an extraordinary wave in a uniaxial crystal with a constant direction of the optical axis [6]:

$$n_{\text{avg}} = n_o n_e / \sqrt{n_o^2 \cos^2\theta + n_e^2 \sin^2\theta}, \tag{2}$$

where the direction of wave propagation is angle $\theta$ to the optical axis. RI (2) turns out to be intermediate between ordinary and extraordinary. For a positive uniaxial crystal, this RI is greater than the ordinary RI and less than the extraordinary RI ($n_o < n_{\text{avg}} < n_e$). In contrast, twisting makes the effective RI less than the ordinary RI or greater than the extraordinary RI ($n_{\text{eff}} < n_o < n_e < n'_{\text{eff}}$).

## MODEL AND TRANSMISSION SPECTRUM

Our structure is a layer of LCs oriented along the surfaces of anisotropic resonator mirrors (Fig. 1). In the simplest case, light is incident normal to the mirror surfaces. The dielectric anisotropic mirrors are uniaxial crystals with the same RI $n_o$ and $n_e$ as the LCs, but the extraordinary axis is twisted through a right angle in the plane of mirrors.

The idea was to preserve both the light's polarization and the Maugin waveguide mode upon reflection [7, 8]. As is well known, reflection reverses the right and left vector triplets, so the isotropic mirror (i.e., the boundary separating the isotropic media) preserves only the linear polarization. All other polarization changes sign, with the right triplet becoming the left triplet and vice versa. This incongruence with its mirror reflection is referred to as chirality. The set of all possible polarizations is usually pictured as Poincare

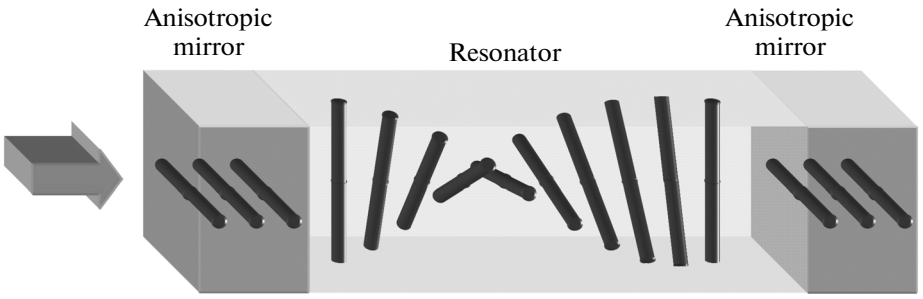


**Fig. 1.** Scheme of a resonator with anisotropic mirrors for registering the effect twisting the optical axis has on the effective refraction index. Rods representing a positive uniaxial crystal are directed along the primary direction of molecular dipoles (the director).

sphere points [2]. A Poincare sphere is a chiral object; its reflection in an isotropic mirror presents it relative to the plane of linear polarizations. However, an achiral mirror that preserves an arbitrary polarization can be created. This requires that we reverse the phase of electric intensity along one and only one of the orthogonal axes upon reflection and the twisting of the wave vector. Polarization is preserved when an RI at the boundary between the media grows along one of main axes and shrinks to the same degree along the orthogonal axis. Our proposed anisotropic mirrors satisfy these conditions. At the same time, the sphere remains chiral with respect to the image transmitted by light waves. A chiral reflection of the image produces a beam of waveguides twisted through 180°.

The helicoid in Fig. 1 shows the period (half-step) of a helical line (a spatial spiral). It is transformed into an infinite helical line by the mirrors and can be considered a chiral photonic crystal with a photonic band gap. Another example of such a structure is cholesteric liquid crystal [1, 9]. Light with, e.g., right circular polarization retains its polarization when reflected from a right-handed cholesteric liquid crystal.

## COMPUTING THE BERREMAN SPECTRUM AND SPATIAL FIELD DISTRIBUTION

Our optical response was calculated using a transfer matrix generalized to an anisotropic medium [10]. The ordinary transfer matrix for a one-dimensional isotropic layered medium measured $2 \times 2$. The matrix was the same for both the vertical and horizontal polarization of light. The waves of vertical and horizontal polarizations interact in an anisotropic medium, leading to the inclusion of two $2 \times 2$ matrices in a transfer matrix measuring $4 \times 4$.

Maxwell's equations for an anisotropic medium can be written in matrix form for matrices measuring $6 \times 6$:

$$\begin{bmatrix} 0 & 0 & 0 & 0 & -\frac{\partial}{\partial z} & \frac{\partial}{\partial y} \\ 0 & 0 & 0 & \frac{\partial}{\partial z} & 0 & -\frac{\partial}{\partial x} \\ 0 & 0 & 0 & -\frac{\partial}{\partial y} & \frac{\partial}{\partial x} & 0 \\ 0 & \frac{\partial}{\partial z} & -\frac{\partial}{\partial y} & 0 & 0 & 0 \\ -\frac{\partial}{\partial z} & 0 & \frac{\partial}{\partial x} & 0 & 0 & 0 \\ \frac{\partial}{\partial y} & -\frac{\partial}{\partial x} & 0 & 0 & 0 & 0 \end{bmatrix} \begin{pmatrix} E_x \\ E_y \\ E_z \\ H_x \\ H_y \\ H_z \end{pmatrix} = \frac{1}{c}\frac{\partial}{\partial t} \begin{pmatrix} D_x \\ D_y \\ D_z \\ H_x \\ H_y \\ H_z \end{pmatrix}$$

$$= \frac{1}{c}\frac{\partial}{\partial t} \begin{pmatrix} \varepsilon_{xx} & \varepsilon_{xy} & \varepsilon_{xz} & \rho_{xx} & \rho_{xy} & \rho_{xz} \\ \varepsilon_{yx} & \varepsilon_{yy} & \varepsilon_{yz} & \rho_{yx} & \rho_{yy} & \rho_{yz} \\ \varepsilon_{zx} & \varepsilon_{zy} & \varepsilon_{zz} & \rho_{zx} & \rho_{xy} & \rho_{zz} \\ 0 & 0 & 0 & \mu_{xx} & \mu_{xy} & \mu_{xz} \\ 0 & 0 & 0 & \mu_{yx} & \mu_{yy} & \mu_{yz} \\ 0 & 0 & 0 & \mu_{zx} & \mu_{zy} & \mu_{zz} \end{pmatrix} \begin{pmatrix} E_x \\ E_y \\ E_z \\ H_x \\ H_y \\ H_z \end{pmatrix},$$

Allowing for changes in medium characteristics in only one direction along the $z$ axis in the steady state lets us simplify the rotor:

$$\begin{pmatrix} 0 & -\frac{\partial}{\partial z} & \frac{\partial}{\partial y} \\ \frac{\partial}{\partial z} & 0 & -\frac{\partial}{\partial x} \\ -\frac{\partial}{\partial y} & \frac{\partial}{\partial x} & 0 \end{pmatrix} = \begin{pmatrix} 0 & -\frac{\partial}{\partial z} & 0 \\ \frac{\partial}{\partial z} & 0 & -ik \\ 0 & ik & 0 \end{pmatrix},$$

where $k$ is the waveguide field vector perpendicular to the $z$ axis. Differentiation disappears in the lower row and we have a linear algebraic equation. This allows us to express unknown components of the electric and

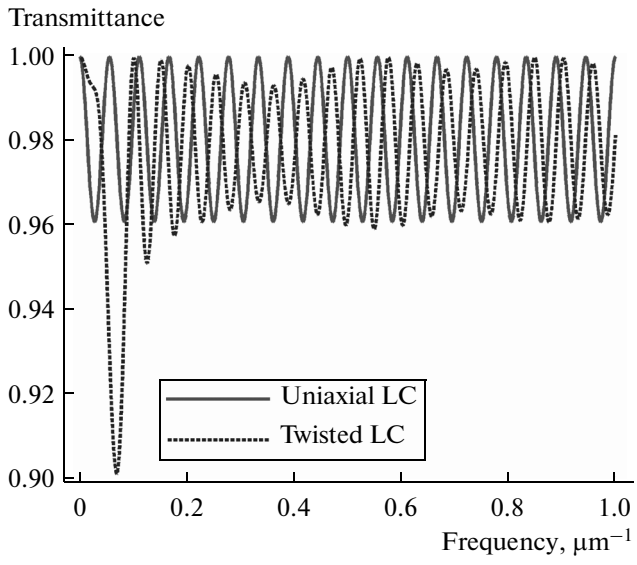


**Fig. 2.** Transmittance spectra of the transverse mode with no twisting and with twisting through 180 degrees (dashed line). Twisting shifts the peaks toward short-wave region; as a result, the effective RI is less than the ordinary RI.

magnetic intensities along the $z$ axis, and to eliminate two equations. The final differential equation describing the propagation of light with frequency $\omega$ along the $z$ axis is written as

$$\frac{d\Psi}{dz} = \frac{i\omega}{c}\Delta(z)\Psi(z), \quad (3)$$

where $\Psi(z) = (E_x, H_y, E_y, -H_x)^T$, $\Delta(z)$ is a Berreman matrix that depends on the dielectric function and wave vector of an incident wave. Computing the field evolution (vector $\Psi(z)$) is reduced to defining the matrix exponent. This nontrivial procedure is executed in such mathematical packages as MatLab:

$$\Psi(z+dz) = \exp\left(\frac{i\omega}{c}\Delta(z)dz\right)\Psi(z), \quad (4)$$

$$\Psi(z) = \hat{T}\Psi(0), \quad (5)$$

where $\hat{T} = \prod_0^z \exp\left(\frac{i\omega}{c}\Delta(z)dz\right)$ is the anisotropic transfer matrix. The first stage of computation is to calculate this matrix.

The second stage is stating boundary problem (5). This differs from the isotropic case, since field vector $\Psi(z)$ is completely unknown at both boundaries. In computations for an isotropic medium in the linear case, the amplitude of transmitted field is assumed to be 1. This condition is not enough in an anisotropic medium, since the field polarization upon exiting cannot be known in advance. We must therefore solve Eq. (5) for four variables, the $xy$-components of transmitted and reflected waves. From this we derive the transmittance and reflection coefficients.

The third stage of computing is to determine the distribution of the field in the depth of the medium. This can be done using the result from the second stage: the value of field vector $\Psi(z)$ at one of the boundaries; for the sake of precision, $\Psi(z = 0)$ upon entry. This value must once again be inserted into Eq. (5) using the partial product of matrix exponents as an anisotropic transfer matrix along the layers, from where they begin to the layer for which the field distribution is computed. In practice, it is impractical to store the partial products determined in the first stage in the PC's memory, so they are calculated again in the third stage.

## RESULTS AND DISCUSSION

Figure 2 shows the transmittance spectra of the transverse mode in an anisotropic resonator. We considered the cases where there was no twisting and when there was twisting through 180 degrees. The spectra were computed using the Berreman method, which generalizes the transfer matrix approach to anisotropic media [10]. Normalized RI $n_o = 0.9$, $n_e = 1.1$ were used in our computations; the resonator length was 10 μm. The twisted structure displays low transmittance at frequencies of ~0.1 $\mu m^{-1}$ corresponding to a wavelength of 10 μm, due to the reflection of light from the structure in photonic band gap.

It can be seen that twisting shifts the peaks toward the shortwave region. At the same time, displacement is greater at the lower frequency. The shortwave shift reflects the decrement in effective RI (1), which becomes lower than the ordinary RI.

The first stage of our theoretical description is determining the parameters of a wave propagating along the helical axis of a twisted LC. When there is no stress, the LC is twisted uniformly and translation-rotational symmetry can be applied. Using the transfer matrix for an anisotropic medium [10], the expression for a wave in the LC is rewritten as

$$\begin{bmatrix} E_x \\ H_y \\ E_y \\ -H_x \end{bmatrix} = A\exp(i(\vec{q}+\vec{\beta})z)\begin{bmatrix} 1 \\ (\vec{q}+\vec{\beta})/\vec{k}_0 \\ -i \\ -i(\vec{q}+\vec{\beta})/\vec{k}_0 \end{bmatrix} + B\exp(i(\vec{q}-\vec{\beta})z)\begin{bmatrix} 1 \\ (\vec{q}-\vec{\beta})/\vec{k}_0 \\ i \\ i(\vec{q}-\vec{\beta})/\vec{k}_0 \end{bmatrix},$$

where $E$, $H$ are the complex intensities of the electric and magnetic fields; $\vec{k}_0 = \omega/c$ is the wave vector in

vacuum; $\vec{\beta} = 2\pi/p$ is the twisting vector of the LC director; $p$ is the step of the LC helix, twisting angle $\varphi(z) = \beta z$. The wave vector in the medium is

$$q^{\pm} = \pm\sqrt{\beta^2 + \varepsilon k_0^2 \pm 2\beta k_0\sqrt{\varepsilon + \delta^2 k_0^2/4\beta^2}}, \qquad (6)$$

where $\varepsilon \pm \delta$ denotes main values of the LC's dielectric permeability tensor. The ratio between the amplitudes of the waves polarized circlewise along the helix is

$$B/A = [(q+\beta)^2/k_0^2 - \varepsilon]/\delta$$
$$= \delta/[(q-\beta)^2/k_0^2 - \varepsilon].$$

Let us consider case $\vec{k}_0 \gg \vec{\beta}$. The high value of wave number $|q^+|$ (6) corresponds to an elliptical wave whose primary polarization is codirectional with the LC director. We shall consider this wave to be nearly longitudinal (an $L$-wave). The low value of wave number $|q^-|$ corresponds to an elliptical wave with primary polarization perpendicular to LC director. We shall consider this wave to be almost transverse (a $T$-wave). Figure 3a shows a $T$-wave computed using the Berreman method for light with a wavelength in vacuum of $\lambda_0 = 200$ nm and with right elliptical polarization $[E_x; E_y] = [0.25i; 1]$, propagating in a uniform medium with RI $n_o = 1.5$ and incident along the normal on an LC cell 1/6 μm thick. The LC on the nearest boundary has planar orientation along the $x$ axis and is twisted clockwise through 45°. The LC's ordinary RI $n_o = 1.2$; its extraordinary RI $n_e = 1.8$. In each layer of the medium, the end of intensity vector of electric field describes a counterclockwise elipse. The major axis of this ellipse is perpendicular to the LC's director. The ellipses of different layers of the LC are shown with thin lines. Looking toward the wave, the intensity rotates clockwise, so it is referred to as right. At a fixed moment in time, the ends of the intensities at different points along the axis form an oblate right helix. In Fig. 3a, there is a corresponding bold line whose ends are distorted as a result of reflection from the boundaries of the LC cell. In image plane ($xy$), the helix assumes the trajectory of a Foucault pendulum. This is an elliptical motion considered in a rotating reference system. The Maugin rotation of the polarization ellipse takes the form of optical activity. However, there is no real optical activity in the LC, and the rotation is due to the turning of the LC director.

Figure 3b compares the dispersion curves of $L$- and $T$-waves obtained using Eq. (6) to the linearly polarized $O$- and $E$-waves ($O$, ordinary; $E$, extraordinary).

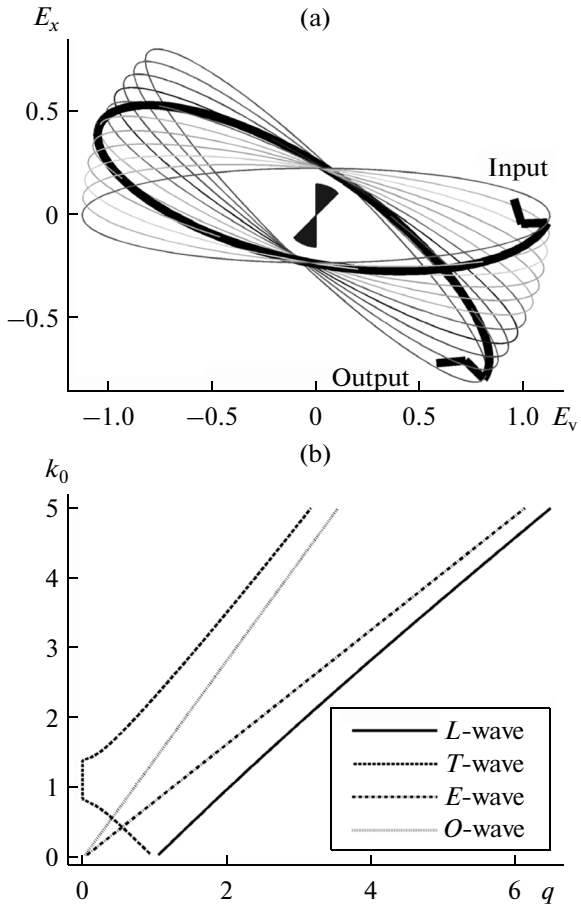


**Fig. 3.** Running wave in a twist-cell. (a) $T$-wave. The bold line represents the many ends of the electric field intensity vectors in each layer of a LC at one moment in time. The thin ellipses are the trajectories of intensities in separate layers of the LC over time. The rotation of the LC director is reflected in the center. (b) Dispersion curve of equation (6). The $L$- and $T$-waves have wave vector $\vec{q}$ outside the range between ordinary and extraordinary ($O$- and $E$-) waves.

## CONCLUSIONS

The shortwave displacement of the considered transverse mode spectrum can only be substantiated theoretically, since it was screened by the quasi-intersection of modes. Observation of the effect twisting has on an effective RI is restricted by the low anisotropy of LCs. High anisotropy can be ensured by an anisotropic nanocomposite consisting of nanosized metal orientationally ordered spherical impurities dispersed in a transparent matrix [11].

## ACKNOWLEDGMENTS

This work was supported by Russian Ministry of Education and Science under the Government program, Project No. 3.1276.2014/K; by the Presidium of the Russian Academy of Sciences, grant nos. 24.29, 24.31; by the Russian Academy of Sciences' Department of Physical Sciences, grant no. III.9.5; by the Siberian Branch of the Russian Academy of Sciences, grant nos. 43, 101; by the Russian Foundation for Basic Research, grant no. 14-08-31248. It was part of a joint project between the Taiwan Ministry of Science

and Technology and the Siberian Branch of the Russian Academy of Sciences.

## REFERENCES

1. Blinov, L.M., *Zhidkie kristally: Struktura i svoistva* (Liquid Crystals: Structure and Properties), Moscow: Librokom, 2013.
2. Klyshko, D.N., *Usp. Fiz. Nauk,* 1993, vol. 163, no. 11, pp. 1–18.
3. Timofeev, I.V., *Sb. tez. dokl. Pervoi vserossiiskoi konferentsii po zhidkim kristallam* (Proc. 1st All-Russian Conf. on Liquid Crystals), Ivanovo, 2012, p. 211.
4. Zhu, X., Huang, Y., and Wu, S.-T., *J. Appl. Phys.*, 2003, vol. 94, no. 5, pp. 2868–2873.
5. Timofeev, I.V., Lin, Y.-T., Gunyakov, V.A., Myslivets, S.A., Arkhipkin, V.G., Vetrov, S.Ya., Lee, W., and Zyryanov, V.Ya., *Phys. Rev. E*, 2012, vol. 85, no. 1, p. 011705(7).
6. Vinogradova, M.B., Rudenko, O.V., and Sukhorukov, A.P., *Teoriya voln* (Waves Theory), Moscow: Nauka, 1979.
7. Timofeev, I.V., Arkhipkin, V.G., Vetrov, S.Ya., Zyryanov, V.Ya., and Lee, W., *Opt. Mater. Express*, 2013, vol. 3, no. 4, p. 496–501.
8. Timofeev, I.V., Arkhipkin, V.G., Vetrov, S.Ya., Zyryanov, V.Ya., and Li, V., *Uchen. Zap. Fiz. Fakult. Mosk. Gos. Univ.*, 2013, no. 5, p. 135052.
9. Shabanov, V.F., Vetrov, S.Ya., and Shabanov, A.V., *Optika real'nykh fotonnykh kristallov: zhidkokristallicheskie- defekty, neodnorodnosti* (Optics of Real Photon Crystals: Liquid Crystal Defects, Inhomogmeities), Novosibirsk: Siberian Branch RAS, 2005.
10. Berreman, D.W., *J. Opt. Soc. Am.*, 1972, vol. 62, no. 4, pp. 502–510.
11. Vetrov, S.Ya., Pankin, P.S., and Timofeev, I.V., *Wave Phenomena*, accepted for publication, 2014.

*Translated by K. Gumerov*